



## UvA-DARE (Digital Academic Repository)

### Influence of feedback in wave based chaotic networks

Sprik, R.

**DOI**

[10.1016/j.procs.2010.04.182](https://doi.org/10.1016/j.procs.2010.04.182)

**Publication date**

2012

**Document Version**

Final published version

**Published in**

Procedia Computer Science

**License**

CC BY-NC-ND

[Link to publication](#)

**Citation for published version (APA):**

Sprik, R. (2012). Influence of feedback in wave based chaotic networks. *Procedia Computer Science*, 1(1), 1625-1633. <https://doi.org/10.1016/j.procs.2010.04.182>

**General rights**

It is not permitted to download or to forward/distribute the text or part of it without the consent of the author(s) and/or copyright holder(s), other than for strictly personal, individual use, unless the work is under an open content license (like Creative Commons).

**Disclaimer/Complaints regulations**

If you believe that digital publication of certain material infringes any of your rights or (privacy) interests, please let the Library know, stating your reasons. In case of a legitimate complaint, the Library will make the material inaccessible and/or remove it from the website. Please Ask the Library: <https://uba.uva.nl/en/contact>, or a letter to: Library of the University of Amsterdam, Secretariat, Singel 425, 1012 WP Amsterdam, The Netherlands. You will be contacted as soon as possible.



International Conference on Computational Science, ICCS 2010

## Influence of feedback in wave based chaotic networks

Rudolf Sprik

*Van der Waals-Zeeman Instituut, Universiteit van Amsterdam, Valckenierstraat 65-67, 1018 XE Amsterdam, The Netherlands*

---

### Abstract

The effective connectivity between input and output channels in complex coupled networks based on the transfer of electro-magnetic waves (RF, microwave or optical) plays an important role in many fields. The transfer of the waves between connected nodes in complex coupled networks is strongly influenced by the presence of non-reciprocal feedback channels with uni-directional amplification. The introduction of such non-reciprocal channels breaks the time reversal invariance of the connectivity matrix between the input and the output channels of the network. The feedback channels are intrinsically changing the spectral properties of the connectivity matrix and hence the associated static and dynamic transfer properties of the ingoing and outgoing ports of the network.

Here we use a random matrix model to represent the complex and fully chaotic network without feedback. Extra feedback connections are introduced that change the reciprocity and time reversal invariance of the reference network and hence the connectivity.

Exploiting a modern electrical engineering description of multi-port complex circuits in terms of the S-matrix of internal multi-port sections, we show by computer simulations the influence of feedback for increasing network complexity. The results are interpreted using a random matrix approach for the multi-port connectivity matrix. The effect of amplifying bi-directional or uni-directional connecting loop on the properties of the resulting S-matrix are computed for increasing network size. The signal transfer capacity of a multi channel the network based on the S-matrix shows for smaller networks a strong influence of the extra connected loop. In particular for the uni-directional amplifying feedback loop.

© 2012 Published by Elsevier Ltd. Open access under [CC BY-NC-ND license](https://creativecommons.org/licenses/by-nc-nd/4.0/).

*Keywords:* multi channel network, signal capacity, wireless, random matrix modeling

---

### 1. Introduction

Complex networks consisting of multiple connected channels with passive and active elements are encountered in many forms. For example the connection of wireless transmitter-to-receiver networks in the presence of active relay station or the connectivity in neural nets with amplification. When the information is transferred over the connected channels in the form of waves with frequency, wavelength and amplitude, the wave propagation characteristics are influencing both static and dynamic properties of the network. For example changing path lengths in the network may alter the transmission by constructive or destructive interference at certain wavelengths. The associated dispersive changes for all participating frequencies will modify the overall temporal response.

---

*Email address:* [R.Sprik@UvA.nl](mailto:R.Sprik@UvA.nl) (Rudolf Sprik)

In the current article we will study the influence of extra channels on waves propagating in a complex network with non-reciprocal and active behavior. As a reference undisturbed network a random matrix representation of the  $n \times m$  connectivity matrix,  $\mathbf{H}$ , between the  $n$  incoming and  $m$  outgoing channels is used. The spectral properties of such systems are well known and characterized by random matrix theory [1, 2, 3]. In particular the maximum obtainable data transfer rates between multiple antenna arrays has been analyzed in detail using Random Matrix Theory to describe a multi-channel extension [4] of the Shannon capacity theory [5] for a single channel. The basis for these approaches is the singular values of  $\mathbf{H}$  (or equivalently the eigenvalues of  $\mathbf{H}^\dagger \mathbf{H}$ ).

To study the effect of a limited number of non-reciprocal and active connections on the transfer in a network we start with a fully random system as described above and connect some input to output channels by a feedback loop (see fig.1). This way the original  $n \times m$  connectivity matrix is reduced to a  $(n - s) \times (m - s)$  matrix if  $s$  channels are connected by a feedback loop. The feedback loop may be just a passive bi-directional loop (i.e. a shunt cable) or may contain e.g. uni-directional amplifiers that break the reciprocity. Since we are interested in the changes in both forward and backward connectivity in the network, the modeling will be done on a square  $n \times n$  matrix where all  $n$  ports can act as input or output. This is different from the usual representation of the connectivity matrix where ports are either input or output, but enables a novel and consistent way to analyze the influence of feedback and symmetry breaking.

## 2. S-parameter matrix description of a complex network

To analyze the complex networks with the additional feedback loops, we use an approach that is common to fully describe input and output characteristics of microwave networks in terms of the so called scattering matrix ( $\mathbf{S}$ -matrix) [6]. With each port connected to the network, the possible incoming and outgoing waves are considered simultaneously. This allows for a detailed analysis of the reciprocity and amplification or attenuation of the network with and without feedback loops.

The  $\mathbf{S}$ -matrix used in electronics for microwave circuits is similar to the  $\mathbf{S}$ - and  $\mathbf{T}$ -matrix formalism developed to describe the physics of wave scattering in classical and quantum mechanics. In both approaches the incoming and outgoing complex amplitudes of the waves are exploited to fully describe the scattering problem [7]. Here we will follow the route developed in electronic engineering for multi-port circuits [8] since it provides a practical scheme to perform computer calculations. Furthermore, the multiport approach is directly usable in measurements of circuits with a network analyzer.

In electrical engineering the  $\mathbf{S}$ -parameter matrix of a  $n$ -multiport circuit,  $\mathbf{S}_{ij}$ , with  $i$  and  $j = 1, \dots, n$  is used to fully characterize a linear system. The matrix elements of  $\mathbf{S}$  describe the voltage ratios of the incoming and outgoing waves for the ports at frequency  $\omega$  and are in general complex dimensionless elements. For example,  $\mathbf{S}_{11}$  is the ratio of the amplitude of the reflected wave and the incoming wave at port-1 and  $\mathbf{S}_{12}$  the ratio of the incoming wave at port-1 and the outgoing wave at port-2. The voltages are referenced to a characteristic impedance of e.g.  $50\Omega$ . Perfect matching of the incoming wave to this impedance means:  $\mathbf{S}_{ii} = 0$ . In a system without dissipation or amplification the  $\mathbf{S}$ -matrix is unitary and in a reciprocal system symmetrical:  $\mathbf{S}_{ij} = \mathbf{S}_{ji}$ . The  $\mathbf{S}$ -matrix of 2, 4 or even higher order multiport systems can be fully characterized by modern vector network analyzers if the correct calibration procedure is followed [6].

Complex coupled multiport systems are combinations of multiport subsections where some of the ports are exposed to the outside and others are connected internally. An example is sketched in Fig.1. Some ports of the multiport systems  $\mathbf{A}$ , and extra section  $\mathbf{C}$  are connected by (perfect and zero delay) cables and are not accessible from the outside. For example ports  $\mathbf{A}_1$  and  $\mathbf{A}_2$  of  $\mathbf{A}$  are accessible from the outside and system  $\mathbf{C}$  is a feedback loop connecting ports  $\mathbf{A}_3$  and  $\mathbf{A}_4$ . The feedback loop in  $\mathbf{C}$  may for instance contain an amplifier that causes this section to be non-reciprocal and non-unitary.

To analyze a combination of multiport systems different approaches are possible. One way is to rewrite the  $\mathbf{S}$ -matrix of each of the sections in terms of a  $\mathbf{T}$ -matrix [6] describing the reflection and transmission of the waves. The complete  $\mathbf{T}$ -matrix of the system is than the product of the  $\mathbf{T}$ -matrices of each of the subsections. Finally transforming the  $\mathbf{T}$ -matrix back to the  $\mathbf{S}$ -matrix gives the results for the complete system. This approach is often used to include the effect of connecting leads in the analysis of 2-port systems. However, finding the transforms for a complex multiport system is tedious. An alternative has been worked out in connection with coupled microwave resonators to perform

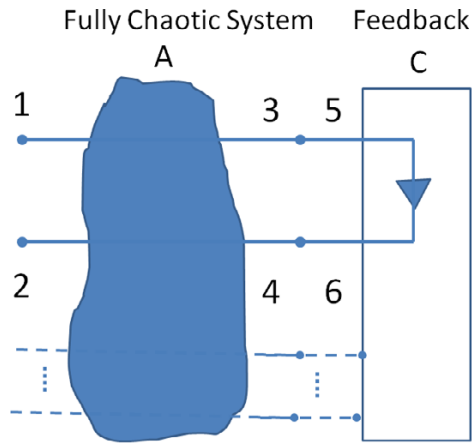


Figure 1: Complex network with feedback elements. Section **A** represents a multiport complex system with 4 leads. Ports **A**<sub>1</sub> and **A**<sub>2</sub> are connected to the outside and ports **A**<sub>3</sub> and **A**<sub>4</sub> are terminated internally by the 2-port feedback loop **C** with ports **C**<sub>5</sub> and **C**<sub>6</sub>. The dashed lines may constitute additional ports and feedback elements.

coupled **S**-parameter calculations [9]. This method uses the **S**-matrices of the subsystems to find the **S**-matrix for all exposed ports directly and is easy to implement in computation. A detailed proof of the validity and a discussion with examples can be found in [9]. Here only a short outline of the method will be given using the case in Fig.1 as an example.

The procedure starts by defining the full sized 6x6 **S**<sub>*f*</sub>-matrix for all ports occurring in the problem (ports 1, ..., 6 in Fig.1 ). Now sections **A** and **C** define a 4x4 and a 2x2 block matrix on the diagonal of **S**<sub>*f*</sub>:

$$\mathbf{S}_f = \begin{pmatrix} \mathbf{A} & 0 \\ 0 & \mathbf{C} \end{pmatrix}.$$

Next a 6x6 permutation matrix **P** is defined that rearranges the order of the ports such that all exposed ports (i.e. **A**<sub>1</sub> and **A**<sub>2</sub>) are in a block matrix at the bottom of the diagonal of **S**<sub>*f*</sub>. In addition a connectivity matrix **F** is defined that indicates which ports are internally connected. In particular for the example the permutation matrix

$$\mathbf{P} = \begin{pmatrix} 0 & 0 & 0 & 0 & 1 & 0 \\ 0 & 0 & 0 & 0 & 0 & 1 \\ 1 & 0 & 0 & 0 & 0 & 0 \\ 0 & 1 & 0 & 0 & 0 & 0 \\ 0 & 0 & 1 & 0 & 0 & 0 \\ 0 & 0 & 0 & 1 & 0 & 0 \end{pmatrix}$$

moves the rows associated with exposed ports **A**<sub>1</sub> and **A**<sub>2</sub> to the bottom rows and the connectivity matrix

$$\mathbf{F} = \begin{pmatrix} 1 & 0 & 0 & 0 & 0 & 0 \\ 0 & 1 & 0 & 0 & 0 & 0 \\ 0 & 0 & 0 & 0 & 1 & 0 \\ 0 & 0 & 0 & 0 & 0 & 1 \\ 0 & 0 & 1 & 0 & 0 & 0 \\ 0 & 0 & 0 & 1 & 0 & 0 \end{pmatrix}$$

specifies the internal connection between ports  $A_3$  and  $A_4$  to  $C$ . After rearrangement the matrix  $G$  describing the coupled system is:

$$G = P^{-1}FS_fP = \begin{pmatrix} G_{11} & G_{12} \\ G_{21} & G_{22} \end{pmatrix}, \quad (1)$$

with  $G_{22}$  a block matrix with dimensions of the total number of exposed ports (i.e. 2x2 in the example),  $G_{11}$  a block matrix with dimensions of the number of unexposed ports and  $G_{12}$  and  $G_{21}$  the cross coupling terms.

The  $S$ -matrix for the exposed ports can be found by solving the linear matrix equation associated with  $G$  by elimination. This leads to an expression of  $S$  in terms of the Schur complement of matrix  $G$  [10]:

$$S = G_{22} + G_{12}(I - G_{11})^{-1}G_{21}, \quad (2)$$

with  $I$  the unit matrix with the same dimensions as  $G_{11}$ .

In particular for the example of a uni-directional amplified loop between port  $A_3$  and  $A_4$  the parameters for  $C$  assuming matched ports are ( $C_{56} = a$ ,  $C_{65} = 0$ ,  $C_{55} = 0$ ,  $C_{66} = 0$ ) and

$$G = \left( \begin{array}{cccc|cc} 0 & 0 & C_{55} & C_{56} & 0 & 0 \\ 0 & 0 & C_{65} & C_{66} & 0 & 0 \\ A_{33} & A_{34} & 0 & 0 & A_{31} & A_{32} \\ A_{43} & A_{44} & 0 & 0 & A_{41} & A_{42} \\ \hline A_{13} & A_{14} & 0 & 0 & A_{11} & A_{12} \\ A_{23} & A_{24} & 0 & 0 & A_{21} & A_{22} \end{array} \right).$$

(The lines indicate the subdivision of  $G$  in sub-blocks).

Using Eq.2 the expression for the  $S$  with feedback becomes [11]:

$$S^{fb} = \begin{pmatrix} A_{11} + A_{13}A_{41}\Gamma & A_{12} + A_{13}A_{42}\Gamma \\ A_{21} + A_{23}A_{41}\Gamma & A_{22} + A_{23}A_{42}\Gamma \end{pmatrix}, \quad (3)$$

with

$$\Gamma = \frac{a}{1 - aA_{43}} \quad (4)$$

characterizing the feedback in the system using an ideal non-reciprocal amplifier with an amplification factor  $a$ . If the input and output ports  $A_1$  and  $A_2$  are matched to  $50\Omega$ , Eq.3 reduces even further ( $A_{11} = A_{22} = 0$ ).

Near poles of  $\Gamma$  when  $aA_{43} \approx 1$  the feedback leads to gain and self-oscillation in the system. The feedback also breaks the reciprocity in the system even if  $A$  by itself is reciprocal as can be seen from the terms in the off diagonal elements in  $S^{fb}$ . In the next section some simulated examples of the influence of the feedback will be presented.

### 3. Numerical random matrix modeling of the feedback

In chaotic and strongly scattering systems with contact leads and reciprocal character the statistical properties of the elements of the  $S^{fb}$ -matrix of the system may be modeled by a random matrix approach [1, 2, 3]. Simulating the consequence of random choices of the matrix elements of e.g.  $A$  in Eq.3 will demonstrate the effect of the fixed feedback loop  $C$ . In the next sections some numerical simulations will be presented.

#### 3.1. Open dissipative $4 \times 4$ network with 1 loop

If system  $A$  in Fig.1 is a chaotic system with reciprocity the elements  $A_{ij} = A_{ji}$  can as a first approach be modeled by independent identical distributions. To represent an open or strongly dissipative network choosing a complex distribution with a constant amplitude and random phase  $\phi$ :

$$A_{ij} = \exp(i2\pi\phi), \quad (5)$$

with  $\phi$  uniform distributed in  $[0, 1)$  gives a good indication of the fluctuations in the transmission at a fixed frequency. The extra terms in Eq.3 due to the feedback  $\Gamma$  specified in Eq.4 will disturb these fluctuations and modify the statistics. Also  $\Gamma$  itself is fluctuating.

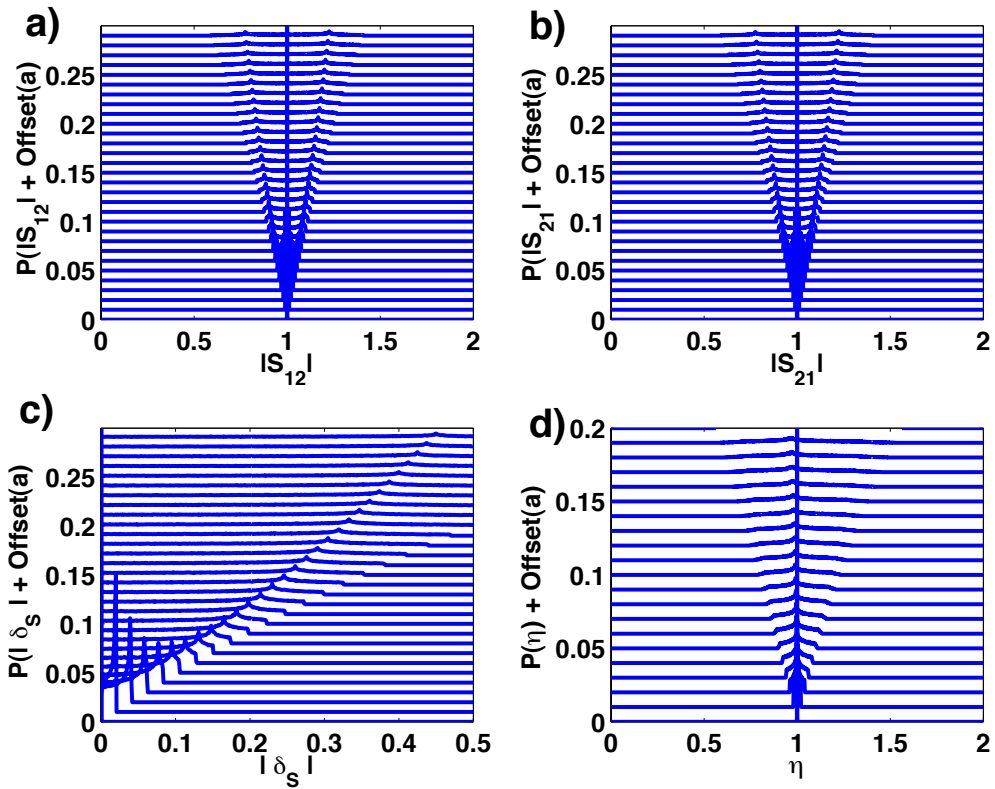


Figure 2: Computer simulation of the feedback model Eq.3 and independent complex Gaussian random terms for  $A_{ij}$  and assuming reciprocity ( $A_{ij} = A_{ji}$ ). The estimate of the probability distribution  $P(|S_{12}|)$  and  $P(|S_{21}|)$  for forward and backward transmission is illustrated in graphs a) and b) for different values of  $a$ . The offset of the curves along the y-axis in the graphs give the value of  $a$  ranging between  $a = 0$  (bottom) to  $a = 0.5$  in steps of 0.05. The graphs c) and d) show the results from the same simulation for the difference parameter  $\delta_s$  (Eq.6) and the fidelity parameter  $\eta$  (Eq.7).

Fig.2.a shows the results of a computer simulation of the probability distribution  $P(|S_{12}|)$  of  $|S_{12}|$  based on a simulation of  $10^5$  randomly chosen realization of  $\mathbf{A}$  and different amplification  $a$  in the feedback loop. On increasing  $a$  in the feedback, the unitary character of  $\mathbf{S}^{fb}$  is disturbed and leads to  $|S_{12}| > 1$  (amplification) or  $|S_{12}| < 1$  (attenuation). The results for  $|S_{21}|$  (Fig.2.b) is similar to the results for  $|S_{12}|$  and do not show right away the effect of the feedback on the reciprocity. To characterize the effect of feedback two different parameters will be used. The first one,  $\delta_S$  quantifies the difference:

$$\delta_S = \langle |S_{12} - S_{21}| / \sqrt{|S_{12}| |S_{21}|} \rangle, \quad (6)$$

where the averaging  $\langle \rangle$  is over all random realizations of  $\mathbf{A}$ . For a reciprocal system  $\delta_S = 0$  as can be seen for the limit  $a = 0$  in Fig.2.c and spreads out rapidly for  $a > 0$ .

Another parameter to characterize reciprocity and reversal time invariance we will use is inspired by the concept of fidelity used in time dependent quantum mechanics problems to characterize the stability of the quantum mechanical wave function against changes [12]. It is in particular useful to compare the time response (or equivalently the wide bandwidth frequency response) in forward or backward evolving wave functions. For now we will define the fidelity,  $\eta$ , for a single frequency as:

$$\eta = \langle |S_{12} S_{21}^*|^2 / \sqrt{|S_{12}|^2 |S_{21}|^2} \rangle. \quad (7)$$

In case of a reciprocal and time reversible system,  $\eta = 1$ , as can be seen in Fig.2.d. Note that the fidelity rapidly changes when the feedback loop with uni-directional amplification is present.

### 3.2. Unitary symmetric $4 \times 4$ network with 1 loop

If the undisturbed part of the network is energy conserving and reciprocal then  $\mathbf{A}$  is a symmetric unitary matrix. In the literature stable algorithms to generate random unitary matrices have been published and are derived from a complex normal distributed random matrix of the same dimensions through a QR-decomposition [13]. For such a unitary matrix  $\mathbf{A}_{US}$   $|\det(\mathbf{A}_{US})| = 1$  and  $\mathbf{A}_{US} = \mathbf{A}_{US}^T$ . Adding the feedback loop will change the symmetry and the unitarity of the resulting  $\mathbf{S}^{fb}$  (Eq.3).

Fig.3 show the results for a simulation with  $\mathbf{A}$  a unitary symmetric ensemble and a feedback loop with a bi-directional amplification ( $C_{55} = 0, C_{56} = C_{65} = a, C_{66} = 0$ ) with  $a$  close to 1. Only for  $a = 1$  the system remains unitary: a small deviation from  $a = 1$  leads to amplification or absorption.

The  $4 \times 4$  network with 1 loop is effectively only one channel with a strength of connectivity proportional to  $|S_{12}|^2$ . The results for the variation of connectivity as function of  $a$  are shown in Fig.4. For the symmetric case and  $a = 1$ , hence  $\mathbf{S}^{fb}$  symmetric unitary, this gives  $\langle |S_{12}| \rangle = 0.5$ . The asymmetric case gives always a lower connectivity than the symmetric case and stays well below 0.5 for  $a = 0.9 \dots 1.1$ . This is a significant effect of the unidirectional connectivity loop associated with the breaking of the reciprocity in the loop and the associated non-unitarity of the loop matrix  $\mathbf{C}$ .

### 3.3. Multi-channel systems with feedback loop

The approach outlined in section 2 can be applied to a multiport network where  $\mathbf{A}$  is a  $n \times n$  random symmetric unitary matrix and with one loop reduces to a  $(n-1) \times (n-1)$  network. Various parameters of the network can be extracted from a random matrix simulation. At the basis of the estimate of the signal transfer capacity is the analysis of Teletar [4, 2]. To estimate the capacity one needs the singular values of the connectivity matrix  $\mathbf{H}$  or equivalently the eigenvalues of  $\mathbf{H}^\dagger \mathbf{H}$ . The so called ergodic transfer capacity  $C_{tr}$  is specified by:

$$C_{tr} = \langle \log_2 \det[1 + \sigma \mathbf{H}^\dagger \mathbf{H}] \rangle, \quad (8)$$

with  $\sigma$  a measure of the signal-to-noise that is available given the transmitter power and noise in the system (a detailed discussion can be found in [2]). For the characterization of the transfer capacity of the simulated networks in the current work we will use only the maximum eigenvalue of  $\mathbf{H}^\dagger \mathbf{H}$  as a measure of the capacity. The connectivity matrix  $\mathbf{H}$  is obtained from  $\mathbf{S}^{fb}$  by assigning the first  $i = 1 \dots [(n-1)/2]$  ports as input and the remaining  $j = [(n-1)/2 + 1] \dots n$  ports as outputs and take  $\mathbf{H}_{ij} = \mathbf{S}_{ij}^{fb}$ .

Fig.5 shows the result for this simulation with  $10^4$  random symmetric unitary realizations. The influence of the extra loop is most noticeable for the smaller networks. In general the uni-directional loop gives lower values, because

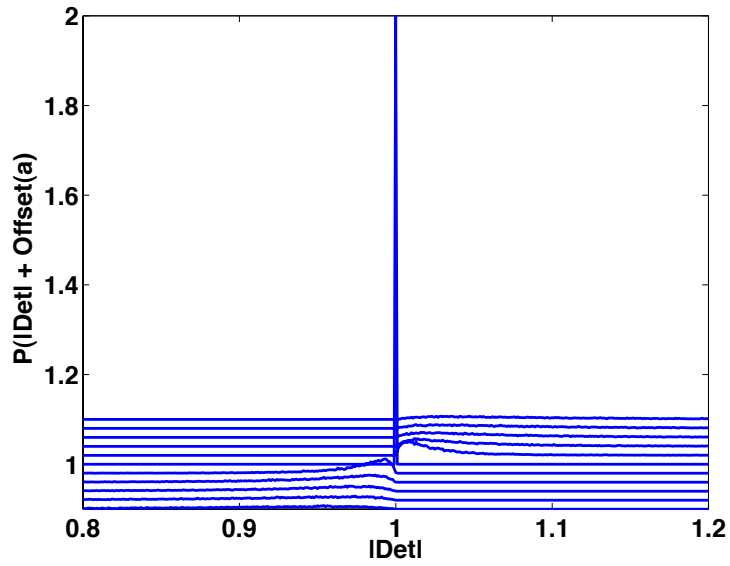


Figure 3: Estimate of the probability distribution  $P(|Det|)$  with  $Det$  the determinant of  $S$  based on the feedback model Eq.3 and a unitary symmetric realizations for  $A$ . The offset of the curves along the y-axis give the value of  $a$  ranging between  $a = 0.9$  (bottom) to  $a = 1.1$  in steps of 0.02.

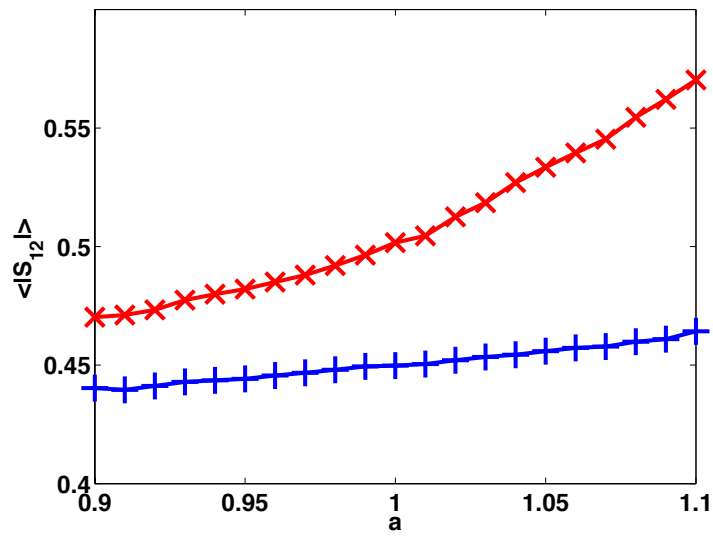


Figure 4: The average transmission  $\langle |S_{12}| \rangle$  as function of  $a$  for a symmetric feedback loop ('x' symbol) and asymmetric ('+' symbol).



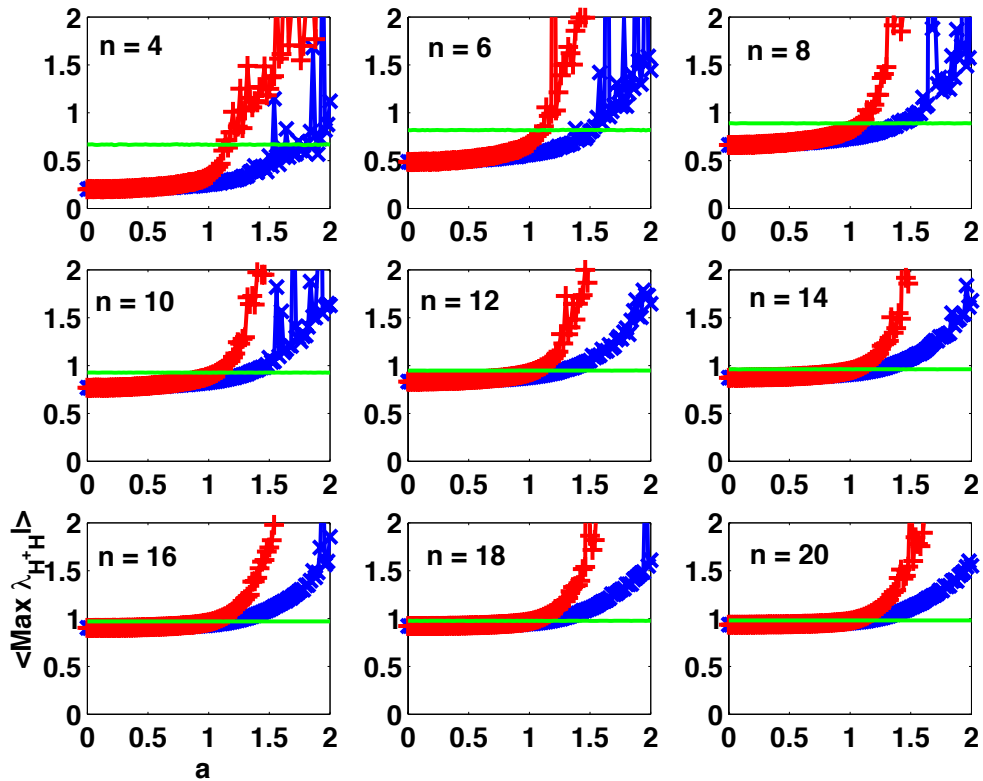


Figure 5: Multiport connectivity: Average maximum eigenvalue  $\lambda_{H^\dagger H}$  for increasing dimensions  $n \times n$  of  $\mathbf{A}$  and one symmetric (+) or uni-directional (x) loop with amplification  $a$ . The reference line (no symbols) is for a system of the same size without feedback loops.

it is always non unitary. For lower  $a$  values the maximum eigenvalue approaches 1 for the largest networks. While for  $a > 1$  an increase can be seen together with larger fluctuations of the average. The results as function of system size are given for  $a = 1$  in Fig.6.

#### 4. Conclusion

In the presented analysis we demonstrated the effect of an extra connecting loop in an otherwise fully chaotic connection. Using the outlined approach, the numerical analysis can be extended to include more loops or even more complex topologies. Also the influence of the loops on the eigenvalue distribution and/or the interval distribution between eigenvalues of the transfer matrix can be tested. To obtain a reliable estimate of the distribution considerably more computation will be required. An analytical treatment of the problem is much harder. Experimental verification of the effects of loops connected to are in progress using microwaves in the 0.5 - 2.5 GHz range in a high quality chaotic cavity [14].

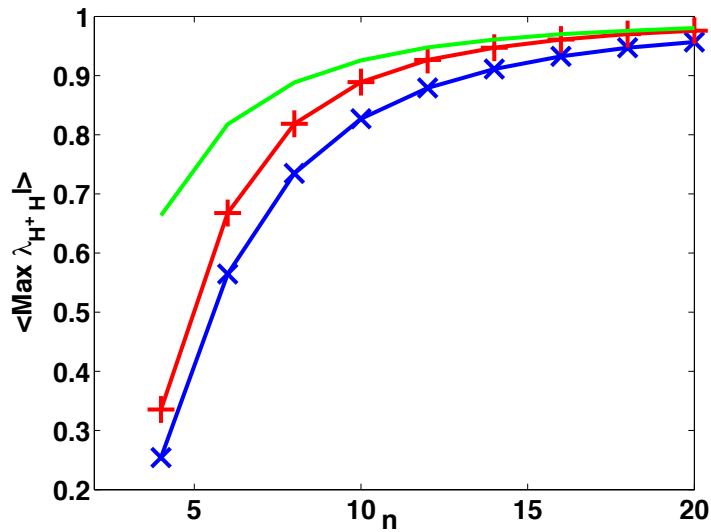


Figure 6: Average maximum eigenvalue  $\lambda_{\mathbf{H}^+ \mathbf{H}}$  as in Fig.5 for increasing dimension  $n \times n$  of  $\mathbf{A}$  and one symmetric (+) or uni-directional (x) loop with amplification  $a = 1$ . The reference line (no symbols, top curve) is for a system of the same  $n \times n$  size without feedback loops.

## References

- [1] M. Mehta, Random Matrices, Third edition. Pure and Applied Mathematics, Elsevier/Academic Press, 2004.
- [2] A. Tulino, S. Verdù, Random matrix theory and wireless communications, Found. Trends Commun. Inf. Theory 1 (2004) 1–.
- [3] R. Sprik, A. Tourin, J. de Rosny, M. Fink, Eigenvalue distributions of correlated multichannel transfer matrices in strongly scattering systems, Phys. Rev. B 78 (2008) 012202.
- [4] E. Telatar, Capacity of multi-antenna gaussian channels, Eur. Trans. Telecom. 10 (1999) 585–, aT & T-Bell Technical Memorandum (1995, see: <http://mars.bell-labs.com>).
- [5] C. Shannon, A mathematical theory of communication, Bell Syst. Tech. J. 27 (1948) 379 and 623.
- [6] Agilent application note AN 1287-3, Applying Error Correction to Network Analyzer Measurements, 2002 (see: <http://www.agilent.com>).
- [7] R. Newton, Scattering theory of waves and particles, second edition, Dover, 2002.
- [8] Agilent application note AN 154, S-parameter design, (2000) (see: <http://www.agilent.com>).
- [9] K. Rothmund, H.-W. Glock, M. Borecky, U. van Rienen, Eigenmode calculation in long and complex rf-structures using the coupled s-parameter calculation technique, ICAP 2000, Darmstadt, and TESLA Report 2000-33, DESY, Hamburg.
- [10] See e.g.: <http://en.wikipedia.org/wiki/Schur-complement>.
- [11] Symbolic manipulations of the matrices performed in Mathematica, Wolfram Research, <http://www.wolfram.com/>. Numerical simulations performed in Matlab.
- [12] H. Stockman, Quantum chaos: an introduction., Cambridge University Press, New York, 1999.
- [13] F. Mazzadri, How to generate random matrices from the classical compact groups, Notices of the AMS 54 (2007) 592.
- [14] R. Sprik, Multi Channel Wave Transfer in Sparsely Connected Systems in Topics on Chaotic Systems, Selected Papers from CHAOS 2008 International Conference, Eds. Christos H Skiadas and Ioannis Dimotikalis and Charilaos Skiadas, p. 323-331, World Scientific (2009).